

This work was written as part of one of the author's official duties as an Employee of the United States Government and is therefore a work of the United States Government. In accordance with 17 U.S.C. 105, no copyright protection is available for such works under U.S. Law.

Public Domain Mark 1.0

<https://creativecommons.org/publicdomain/mark/1.0/>

Access to this work was provided by the University of Maryland, Baltimore County (UMBC) ScholarWorks@UMBC digital repository on the Maryland Shared Open Access (MD-SOAR) platform.

Please provide feedback

Please support the ScholarWorks@UMBC repository by emailing scholarworks-group@umbc.edu and telling us what having access to this work means to you and why it's important to you. Thank you.

SPECTRAL EXPONENTS OF KINETIC AND MAGNETIC ENERGY SPECTRA IN SOLAR WIND TURBULENCE

J. J. PODESTA, D. A. ROBERTS, AND M. L. GOLDSTEIN

NASA Goddard Space Flight Center, Laboratory for Geospace Physics, Heliosphysics Science Division,
 Greenbelt, MD 20771; jpodesta@solar.stanford.edu

Received 2006 October 3; accepted 2007 April 25

ABSTRACT

Kinetic and magnetic energy spectra in the ecliptic plane near 1 AU are found to exhibit different power-law behaviors in the inertial range, with the magnetic spectrum often having a power-law exponent near $5/3$ and the kinetic energy spectrum often having a power-law exponent near $3/2$ (the inertial range extends from approximately 5×10^{-4} to 10^{-1} Hz). The total energy, kinetic plus magnetic, has a power-law exponent that lies between $3/2$ and $5/3$, with a value near 1.6. The Alfvén ratio, the ratio of kinetic to magnetic energy, is found to be a slowly increasing function of frequency in the inertial range, increasing from roughly 0.5 to 0.9 in the frequency range from 10^{-3} to 10^{-1} Hz. These conclusions are based on the analysis of four distinct time intervals of solar wind magnetic field and plasma data obtained by the *Wind* spacecraft near the end of solar cycle 22 and at different times throughout solar cycle 23. Three 54 day intervals and one 81 day interval are used to compute power spectra in the range from 10^{-5} to 1.7×10^{-1} Hz. Power-law exponents are estimated from linear least-squares fits to the logarithm of the power spectral density versus the logarithm of the frequency over the frequency interval from 10^{-3} to 10^{-2} Hz. To prevent errors due to spectral aliasing, the last decade of the spectrum is omitted from the calculation of the power-law exponents. The results show that a measurable difference exists between the power-law exponents of velocity and magnetic field fluctuations and that this difference persists throughout the solar cycle.

Subject headings: solar wind — turbulence

1. INTRODUCTION

Podesta et al. (2006) have recently shown an example in which the power spectrum of solar wind velocity and magnetic field fluctuations display inertial range power-law exponents near $3/2$ and $5/3$, respectively. The purpose of the study described here is to show that these two power laws are typical of velocity and magnetic field fluctuations in the ecliptic plane near 1 AU.

Past studies of solar wind fluctuations have usually focused on the magnetic field fluctuations, due to their importance in cosmic-ray transport and because of the availability of high time resolution magnetometer measurements. High time resolution plasma measurements (protons and ions) that are sufficient to resolve a significant fraction of the inertial range became available with the launch of *Voyager 1* and *Voyager 2* in 1977, but only during the first few months of the mission and with sparse coverage. The approximately 12 s *Voyager* data represents a modest improvement over the 41.5 s plasma data from *Helios*. Nearly continuous 3 s plasma measurements became available with the launch of the *Wind* spacecraft in 1994. However, detailed comparisons of velocity and magnetic field power spectra at the high-frequency end of the turbulent inertial range have not received careful study until recently.

Such studies are important to improve observational knowledge of the turbulence and for comparison with turbulence theory. Resistive magnetohydrodynamics (MHD) has long been considered a reasonable first approximation for the description of solar wind turbulence (Matthaeus & Goldstein 1982; Barnes 1983; Marsch 1991; Burlaga 1995). Computer simulations of incompressible MHD turbulence in a periodic three-dimensional cube, an idealized high Reynolds number model, have not produced a unified view regarding the power-law exponents of the energy spectrum (Verma et al. 1996). Under different conditions, values near *both* $5/3$ (Biskamp & Müller 2000; Müller & Biskamp 2000;

Haugen et al. 2003, 2004a, 2004b; Haugen & Brandenburg 2004; Alexakis et al. 2005; Mininni et al. 2005; Mininni & Montgomery 2005) and $3/2$ (Cho & Vishniac 2000; Maron & Goldreich 2001; Boldyrev et al. 2006; Mason et al. 2006) have been reported in the literature. Moreover, the value of the exponent, like the degree of anisotropy, depends on the strength of the background magnetic field (Müller et al. 2003; Müller & Grappin 2005). Even though the numerical models have improved significantly over the last decade, the theoretical picture is still far from clear.

Currently, the parameters of these simulations are not designed for solar wind studies, and careful comparisons between solar wind observations and specifically designed MHD turbulence simulations are needed. Solar wind simulations performed by Goldstein et al. (1999) generated a spectral exponent approximately equal to $5/3$ for the power in magnetic field fluctuations, but the simulations were limited to an energy cascade of only about one decade and could not distinguish precisely between $3/2$ and $5/3$. Because high Reynolds number simulations may now be able to reach the spatial resolutions required to estimate theoretical power-law exponents, it is an opportune time to perform detailed comparisons between theory and observation. The observations described in this paper should provide a useful baseline for such comparisons.

The contents of this paper are as follows. Section 2 provides an overview of the data selected for this study. Section 3 describes the procedures used to analyze the data. Section 4 presents the results of the analysis. Section 5 contains conclusions and suggestions for future work.

2. DATA SELECTION

The data employed in this study are identified in Table 1. The record length is chosen to be as long as possible. It is desirable that the record length be greater than two solar rotations to ensure

TABLE 1
TIME INTERVALS EMPLOYED IN THE ANALYSIS

Interval	Start Date	End Date	Duration (days)	B Samples	v Samples	Sampling Time (s)
1.....	1995 May 23 00:00:00	1995 Jul 16 00:00:00	54	1555200	1545628	3.018582
2.....	1997 Dec 14 05:52:18	1998 Feb 06 08:03:37	54	1557826	1556888	3.001808
3.....	2000 Nov 15 00:00:00	2001 Feb 04 00:00:00	81	2332800	2277004	3.073512
4.....	2003 Jun 11 02:11:00	2003 Aug 03 22:41:00	53.854	1551020	1534080	3.033087

good statistics for the power spectral estimates and, consequently, small error bars on the resulting spectra. The intervals in Table 1 were also chosen because they are devoid of large data gaps, that is, data gaps with a duration greater than approximately 1 hr. As shown in Table 1, there are three 54 day intervals, each lasting for two solar rotations, and one 81 day interval that lasts for three solar rotations (one solar rotation is approximately 27 days).

The time of occurrence of the four time intervals within the solar cycle are shown in Figure 1. One time interval occurs around solar minimum, one around solar maximum, one during the ascending phase of the cycle, and one during the descending phase of the cycle. These four intervals should provide a reasonable sample of solar wind conditions at any time during the cycle. None of the intervals contain any large CMEs, shocks, or extreme events, such as the Halloween storms of 2003.

The data employed in this study consist of 3 s plasma moments computed onboard the *Wind* spacecraft by the three-dimensional plasma instrument (3DP; Lin et al. 1995) and 3 s averages of magnetic field data from the *Wind* MFI instrument (Lepping et al. 1995).¹ The plasma data consists of the proton bulk velocity vector v and the proton number density n_p . The sampling time (the time between measurements) for the 3DP data is not exactly 3 s

¹ These data are freely available on the internet from NASA's CDAWeb service at <http://cdaweb.gsfc.nasa.gov>.

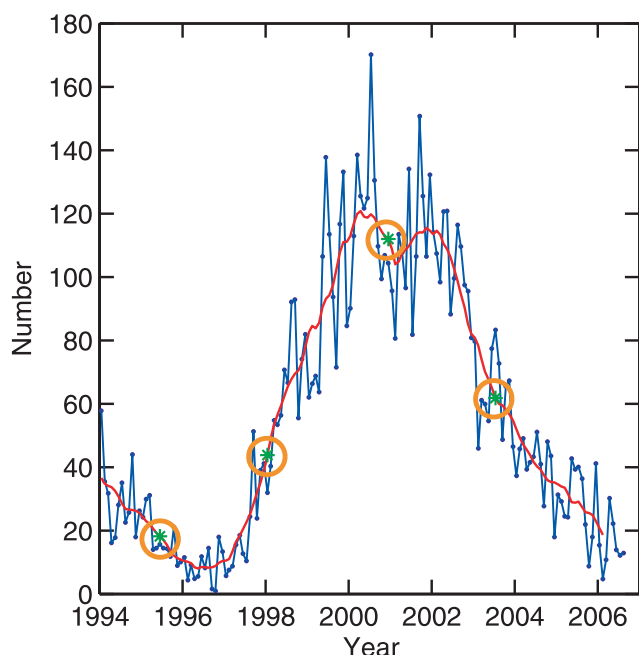


FIG. 1.—Zurich sunspot number and monthly and smoothed data, for solar cycle 23. The circles indicate the four time intervals listed in Table 1.

and changes due to slow changes in the spin rate of the spacecraft. The vector magnetic field data B has an exact 3 s sampling rate, since the data set is composed of 3 s averages processed on the ground from the original magnetometer data, which has a sampling rate of 11 or 22 vectors per second. All data were acquired when the spacecraft was outside the influences of the Earth's magnetosphere.

3. ANALYSIS TECHNIQUES

The plasma data set is sampled once during each revolution of the spacecraft and has a mean sampling time t_s , indicated in Table 1. The magnetic field data set consists of 3 s averages and therefore has a sampling time slightly different from that of the plasma data set. Consequently, the kinetic and magnetic energy spectra are computed separately. Prior to any processing, the data are inspected for outliers and potentially “bad” data points, and a negligibly small number of such points are deleted from the time series. Data gaps and missing data are then linearly interpolated to create a time series without any missing values. This is necessary for processing using Fourier FFT techniques.

Power spectra are computed by means of a smoothed periodogram as described, for example, in chapter 6 of Percival & Walden (1993), where the technique is called a lag window spectral estimator with a Papoulis lag window. The method is briefly described as follows. The mean is subtracted from the data, the length of the data record is doubled by zero padding, the FFT is applied, and the resulting periodogram is smoothed by convolution with a Papoulis smoothing window. Due to the large dynamic range in turbulence spectra, the smoothing is performed with a frequency-dependent bandwidth Δf , given by $\Delta f = f/10$, where f is the frequency in Hz. Thus, the bandwidth is constant with respect to the variable $\log(f)$, and for this reason it is sometimes called logarithmic smoothing. No data tapering is used, because due to the large sample size, the bias error without tapering is small (Podesta 2006). Note that all frequency spectra are measured with respect to the reference frame of the spacecraft.

Differences in the values of the time series at the endpoints of the time interval create “jumps” in the time series when it is periodically continued (due to the FFT). It was verified that these jumps do not affect the power spectra computed here, by computing spectra both with and without removal of the jumps. The jumps were removed by subtracting a line that intersects the initial and final values of the time series, a form of “detrending.” All the spectra employed in the analysis in this paper were obtained without detrending.

The velocity and magnetic field spectra are computed from the time series $v(t)$ and $B(t)$, where v is the proton velocity, B is the magnetic field vector, and the field vectors are measured in geocentric solar ecliptic coordinates (GSE coordinates), in which the x -axis is directed from the earth to the Sun, the z -axis is directed perpendicular and northward with respect to the ecliptic plane, and the y -axis completes the right-handed triple (x, y, z) . The power spectra for each of the three Cartesian vector components

are summed together to obtain the total power. To measure the kinetic energy spectrum, it is necessary to incorporate the density fluctuations into the calculation in an appropriate way.

The instantaneous kinetic energy density in the solar wind frame is defined by

$$\frac{1}{2} \rho(t) |\mathbf{v}(t) - \bar{\mathbf{v}}|^2, \quad (1)$$

where ρ is the mass density, $\bar{\mathbf{v}}$ is the average solar wind velocity, and $|\mathbf{v}|^2 = \mathbf{v} \cdot \mathbf{v}$. Therefore, an appropriate way to compute the kinetic energy spectrum is to compute the power spectrum of the variable

$$\rho^{1/2}(t) [\mathbf{v}(t) - \bar{\mathbf{v}}], \quad (2)$$

where $\bar{\mathbf{v}}$ is the average solar wind velocity over the time interval being analyzed. In this way, the density fluctuations are taken into account in the plasma kinetic energy. The solar wind mass density is computed as

$$\rho(t) = 1.17 m_p n_p(t), \quad (3)$$

where $n_p(t)$ is the proton number density, m_p is the proton mass, and the factor 1.17 accounts for the contribution from the mass of the alpha particles, assuming that $n_p/n_\alpha = 24$. A more complete computation would employ the measured densities and velocities of the alpha particles, but this was not attempted here. This could have a significant effect on the results below, since the density of alpha particles is known to be highly variable (Borrini et al. 1983). This is an important line of investigation for future research.

4. RESULTS

4.1. Magnetic and Kinetic Energy Spectra

Results for the power spectra of velocity and magnetic field fluctuations for the 81 day interval, interval 3, are shown in Figure 2. The 99% confidence intervals are negligibly small for frequencies larger than approximately 7×10^{-4} Hz. Therefore, the error bars on the spectra can be neglected when computing power-law exponents at frequencies greater than 7×10^{-4} Hz. Aliasing errors are on the order of 200% for frequencies near the Nyquist frequency 1.6×10^{-1} Hz and become negligible for frequencies less than $f_{\text{NQ}}/10$, where f_{NQ} is the Nyquist frequency (Podesta et al. 2006). Therefore, power-law exponents can be computed without aliasing errors for frequencies between approximately 7×10^{-4} and 1.5×10^{-2} Hz.

The power-law exponent is obtained from a linear least-squares fit of $\log(P)$ versus $\log(f)$, where P is the smoothed power spectral density. The fit is performed over the frequency interval from 10^{-3} to 10^{-2} Hz. When the left endpoint of the interval is varied from 7×10^{-4} to 1.5×10^{-3} Hz and the right endpoint of the interval is varied from 7×10^{-3} to 1.5×10^{-2} Hz, the measured power-law exponent typically varies by 1%. The variations obtained in this way are comparable to but always less than the error estimates in Table 2. The error estimates shown in Table 2 are 99% confidence intervals based on linear regression analysis and have been rounded up in every case. Because the difference between the spectral exponents 1.52 and 1.66 in Figure 2 is much greater than the experimental uncertainties, this difference is caused by the turbulence itself.

It is important to establish whether the power-law exponents of velocity and magnetic field fluctuations in Figure 2 are typical

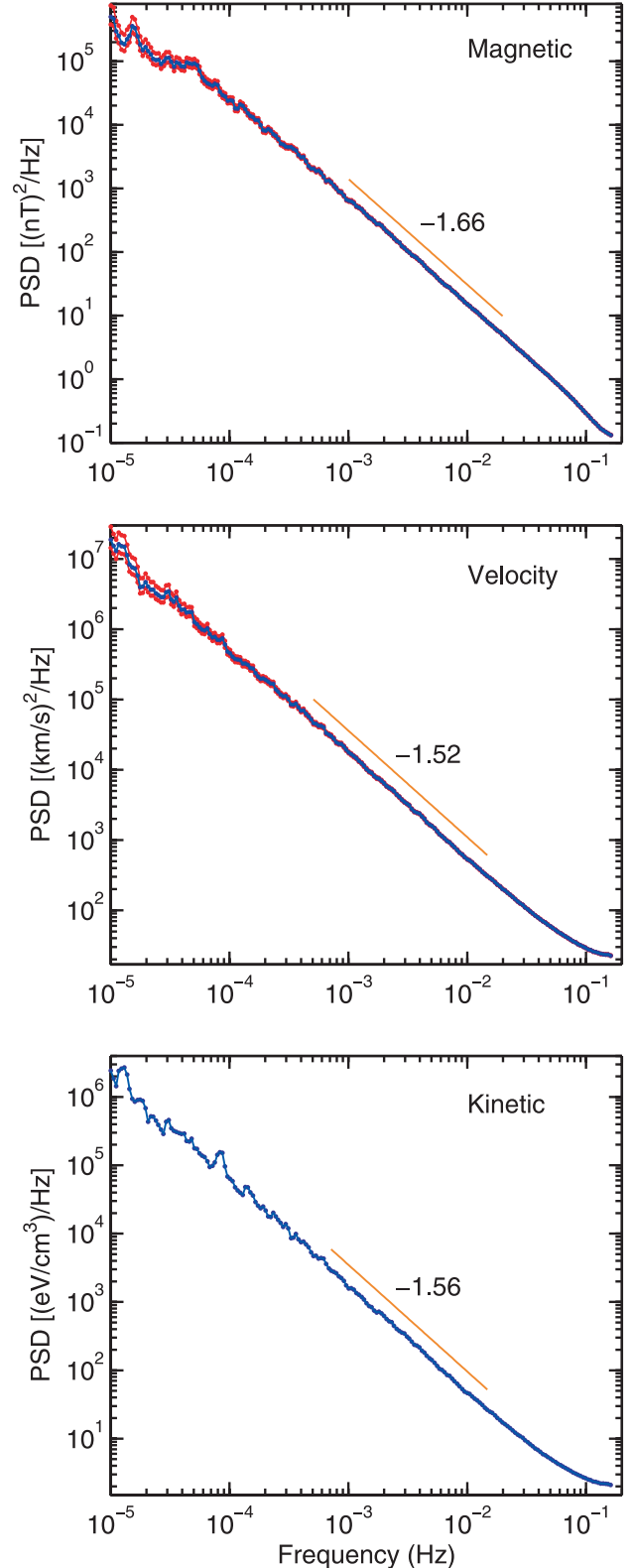


FIG. 2.—Magnetic energy spectra, velocity spectra, and kinetic energy spectra (blue lines) for the 81 day interval, interval 3 in Table 1. The 99% confidence limits (red lines) and least-squares fit (orange lines) are also shown.

of the solar wind or just a one-time observation that is not repeatable from one measurement interval to the next. The results of the analysis of four separate data records shown in Table 2 confirm that this is a repeatable result: the power-law exponents of velocity and magnetic field fluctuations often have values near 3/2

TABLE 2
POWER-LAW EXPONENTS AND ALFVÉN RATIO

Interval	Magnetic	Velocity	Kinetic	E	Alfvén Ratio
1.....	1.66 ± 0.02	1.50 ± 0.02	1.50 ± 0.02	1.60 ± 0.02	0.5–1.1
2.....	1.72 ± 0.02	1.59 ± 0.02	1.59 ± 0.02	1.68 ± 0.02	0.4–0.85
3.....	1.66 ± 0.01	1.52 ± 0.02	1.57 ± 0.03	1.63 ± 0.02	0.5–0.8
4.....	1.58 ± 0.02	1.50 ± 0.02	1.51 ± 0.02	1.55 ± 0.02	0.6–0.85

NOTES.—The power-law exponents have been obtained from fits over the frequency interval $10^{-3} \leq f \leq 10^{-2}$ Hz. The indicated errors are 99% confidence limits, not standard deviations. The Alfvén ratio represents an extrapolation over the interval $10^{-3} \leq f \leq 10^{-1}$ Hz, as explained in the text. The total energy E is the sum of the kinetic plus magnetic energies.

and 5/3, respectively, throughout the solar cycle. This is the principal result of this study.

The kinetic energy spectrum computed from the time series in equation (2) is shown in the lower plot in Figure 2. The fact that the exponent 1.57 of the kinetic energy spectrum is greater than the exponent 1.52 of the velocity spectrum is due to the influence of density fluctuations. Density fluctuations cause the kinetic energy spectrum to decrease more rapidly than the velocity spectrum. If the plasma were incompressible (constant density), then the velocity spectrum and kinetic energy spectrum would both have the same power-law exponents. Thus, plasma compressibility significantly effects the kinetic energy spectrum of interval 3. This has important consequences for the Alfvén ratio. For the other three intervals, the difference between the power-law exponents of the kinetic energy and velocity spectra is almost negligible (see Table 2). For these three intervals, density fluctuations do not significantly affect the power-law exponents of the kinetic energy spectrum.

4.2. Alfvén Ratio

To compare the amplitudes of kinetic and magnetic energy spectra, the magnetic energy spectrum is converted to units of an energy density by simply dividing by the permeability of free space, μ_0 (SI units). The Alfvén ratio, the ratio of the kinetic to

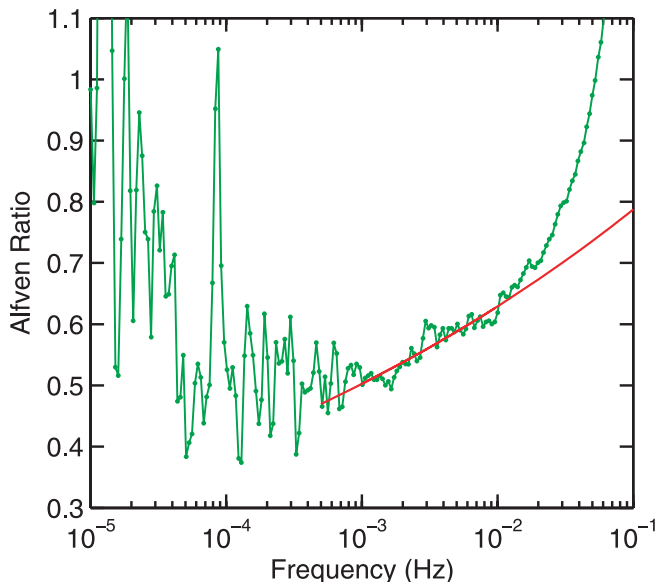


FIG. 3.—Alfvén ratio (green lines) for the 81 day interval, interval 3 in Table 1. The least-squares fit (red lines) over the interval 10^{-3} – 10^{-2} Hz is extrapolated to higher frequencies.

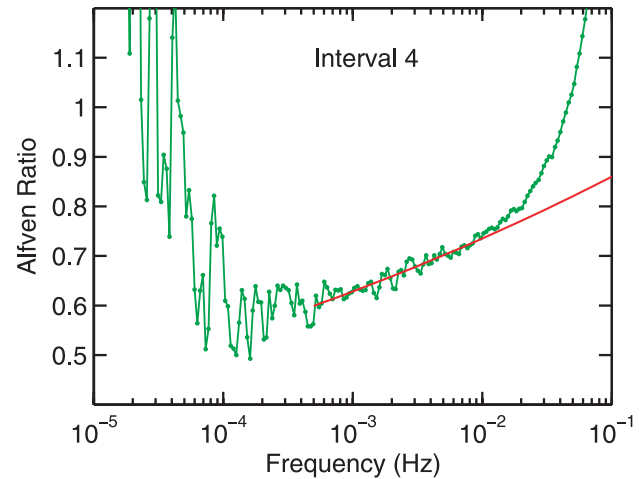
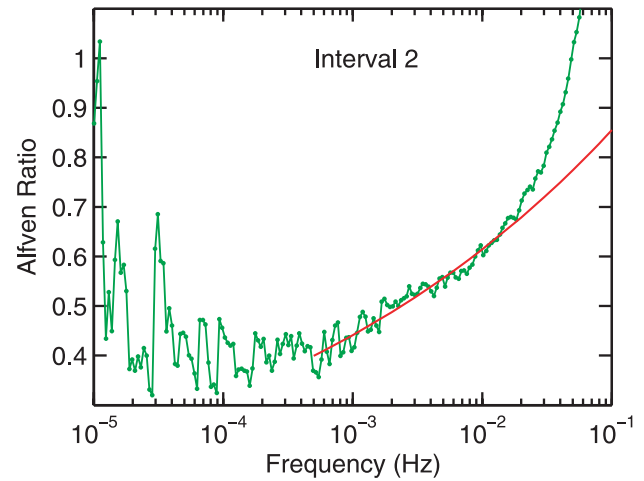
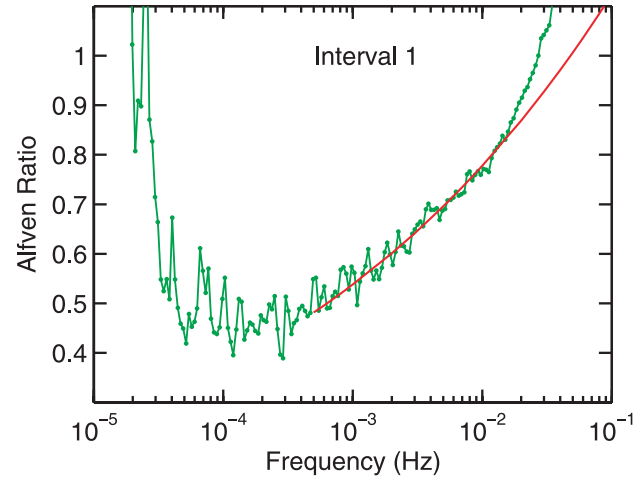


FIG. 4.—Alfvén ratio (green lines), the ratio of kinetic to magnetic energy spectra, for the remaining intervals in Table 1. The least-squares fit (red lines) over the interval 10^{-3} – 10^{-2} Hz is extrapolated to higher frequencies.

magnetic energy spectra, is shown in Figure 3. The Alfvén ratio is a slowly increasing function throughout the inertial range. The rapid rise at high frequencies is not a real effect, but is caused by aliasing in the kinetic energy spectrum. Note from Figure 2 that the magnetic energy spectrum does not appear to exhibit aliasing.

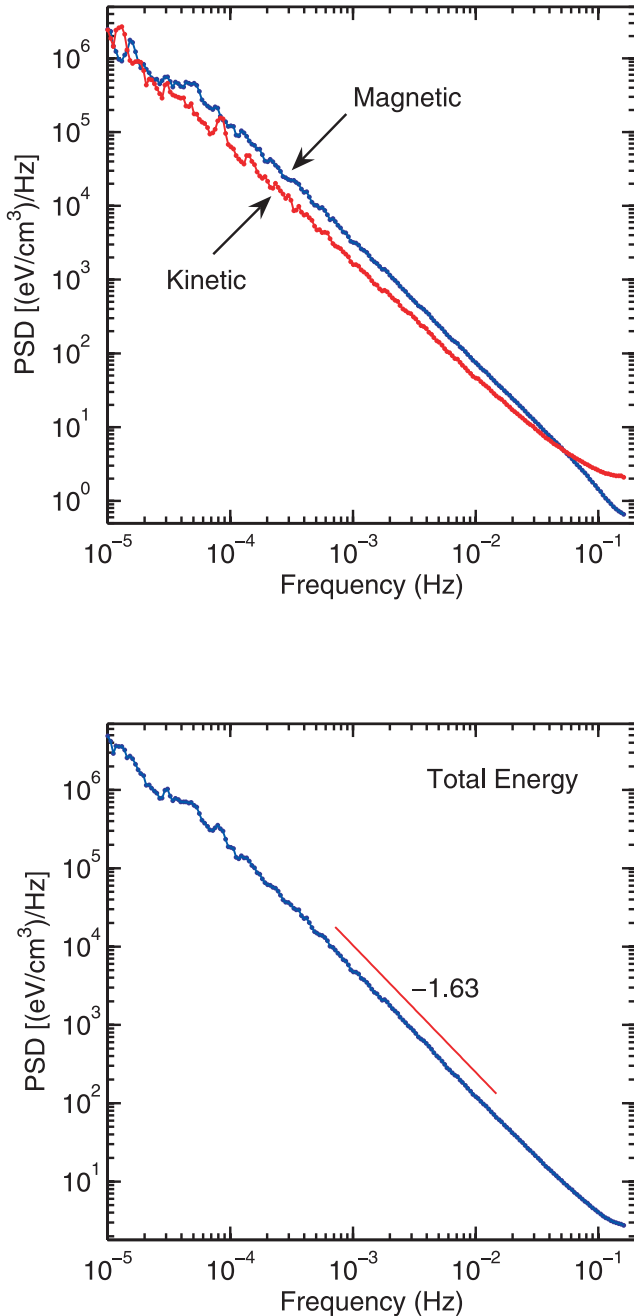


FIG. 5.—Kinetic and magnetic energy spectra (*top panel*) and the total energy (*bottom panel*) for the 81 day interval, interval 3 in Table 1.

This is because the magnetic field data are 3 s averages derived from the original 11 Hz magnetometer data. Only the velocity and kinetic energy spectra display aliasing.

To eliminate aliasing effects from the Alfvén ratio, a linear least-squares fit to the Alfvén ratio is performed over the interval 10^{-3} – 10^{-2} Hz (on a log-log plot). The resulting power-law exponent is 0.1, which is approximately equal to the difference between the power-law exponents for the kinetic and magnetic energies, as it should be. This power law is then extrapolated to higher frequencies to display the trend. The extrapolated Alfvén ratio in Figure 3 is seen to rise from around 0.5 at the lower end of the inertial range to 0.8 at 10^{-1} Hz. The dissipation range of the magnetic spectrum occurs near 5×10^{-1} Hz (Leamon et al. 1998), and the dissipation range of the kinetic energy spectrum

has never been measured, but is also believed to occur near this frequency. Note that the Alfvén ratio (*green line*) starts to deviate from the trend (*red line*) at around 1.5×10^{-2} Hz. This is precisely the point $f_{NQ}/10$ where aliasing errors in the kinetic energy spectrum are expected to increase, suggesting that the sudden rise at high frequencies is due to aliasing.

A similar behavior of the Alfvén ratio in the inertial range and its extrapolation to 10^{-1} Hz is found in each of the four intervals studied, as shown in Figure 4. The observed trend of the Alfvén ratio in the frequency range from 5×10^{-4} to 10^{-1} Hz is listed in Table 2. Hence, the observed behavior is believed to be typical of the solar wind in the ecliptic plane near 1 AU at all times throughout the solar cycle. These results are consistent with those of previous studies, including Matthaeus & Goldstein (1982), Roberts et al. (1987, 1990), Marsch & Tu (1990), Goldstein et al. (1995), and Podesta et al. (2006).

It is interesting that the magnitude of the Alfvén ratio is significantly affected by density fluctuations. Comparisons between the Alfvén ratio obtained using the average density times the velocity spectrum (density fluctuations omitted) and the Alfvén ratio obtained using the kinetic energy spectrum (density fluctuations included) show differences of approximately 10%–30% throughout the inertial range for the four intervals studied here. Therefore, it is important to take density fluctuations into account to accurately compute the Alfvén ratio in the inertial range. It is also noteworthy that in the case of interval 3, the incorporation of density fluctuations into the kinetic energy spectrum causes the Alfvén ratio to increase more slowly than it would if density fluctuations were omitted. This is because the kinetic energy spectrum for interval 3 decreases more rapidly than the velocity spectrum, as shown in Table 2.

4.3. Total Energy

The total energy spectrum is the sum of the kinetic and magnetic energy spectra. By inspection of simultaneous plots of the kinetic and magnetic energy spectra in Figure 5, one can infer that the power-law exponent of the total energy lies between the power-law exponents of the kinetic and magnetic energy spectra (because the sum is twice the average). This is born out by the linear fit shown in the bottom plot of Figure 5, which yields the power-law exponent 1.63. The same behavior is found in each of the four time intervals shown in Table 2. Because the magnetic energy is dominant at small scales, the exponent for the total energy is closer to that of the magnetic energy spectrum than that of the kinetic energy spectrum. One may conclude that at 1 AU, the total energy spectrum of solar wind turbulence has a power-law exponent that lies between that of the kinetic and magnetic energy spectra with a value that lies roughly near 1.6.

5. DISCUSSION AND CONCLUSIONS

The analysis of solar wind power spectra presented here shows that the power-law exponents of velocity and magnetic field fluctuations often have values near $3/2$ and $5/3$, respectively. The kinetic energy spectrum has a power-law exponent that is slightly greater than or equal to $3/2$, due to the effects of density fluctuations. Density fluctuations are found to have a significant effect on the kinetic energy spectrum and the Alfvén ratio. When the velocity spectrum is multiplied by the average density of the measurement interval, the resulting proxy for the kinetic energy spectrum is roughly 5%–30% greater over the frequency interval from 10^{-3} to 10^{-2} Hz than the actual kinetic energy spectrum computed according to equation (2). Therefore, the incorporation of density fluctuations into the kinetic energy spectrum by means of

equation (2) is necessary to obtain an accurate Alfvén ratio. The results of this study suggest that the Alfvén ratio usually remains below unity throughout the inertial range, a result that is consistent with that of previous investigators, including Matthaeus & Goldstein (1982), Roberts et al. (1987, 1990), Marsch & Tu (1990), and Goldstein et al. (1995).

In this paper, kinetic and magnetic energy spectra were computed in terms of the energy per unit volume. If the spectra were instead computed in terms of the energy per unit mass, then the results would be slightly different. For example, the velocity spectrum (energy per unit mass) and the kinetic energy spectrum (energy per unit volume) in Figure 2 have different power-law exponents. It would be of interest to see how the Alfvén ratio changes when the power spectra of velocity and magnetic field fluctuations are computed in terms of energy per unit mass, even though we do not expect to see much difference. This can be checked by computing power spectra based on the variables $v(t)$ and $B(t)/\rho^{1/2}(t)$, as is the usual practice in solar wind studies (Marsch 1991; Tu & Marsch 1995; Bruno & Carbone 2005). Any resulting changes in the spectra and Alfvén ratio may be relevant for comparison with theory.

The results presented in this paper are significant because they extend the results of previous investigations to higher frequencies and clearly demonstrate the differences between the spectral exponents of kinetic and magnetic energy. In the future, it would be of interest to extend the analysis presented here to a larger number of time intervals and to other radial distances. It is also

important to take into account the contributions of the alpha particles to both the bulk plasma velocity and the mass density. This may significantly change the results reported here and so is an important avenue of investigation for future research.

In the future, it would also be important to extend solar wind turbulence measurements to smaller scales. To achieve this there is a need for high time resolution simultaneous plasma and magnetic field measurements with subsecond sampling times. If the 3 s sampling time of current-day plasma measurements is reduced to 0.1 s in future instrumentation, a reduction by a factor of 30, then important unresolved issues in solar wind turbulence research could be addressed. The most important issue is the direct measurement of the onset of the dissipation range for velocity fluctuations, a measurement that cannot be performed using existing instrumentation. Plasma measurements with reduced quantization noise are also urgently needed.

We are grateful to Len Burlaga for his careful reading of the manuscript and for several helpful suggestions. We thank Peter Schroeder at Berkeley Space Sciences Laboratory for his assistance with the 3DP data. We gratefully acknowledge Ron Lepping, the principal investigator of *Wind* MFI, and Robert Lin, the principal investigator of *Wind* 3DP, for the use of their data. The sunspot data was provided by R. A. M. Van der Linden at the Royal Observatory of Belgium (<http://sidc.oma.be/html/sunspot.html>).

REFERENCES

- Alexakis, A., Mininni, P. D., & Pouquet, A. 2005, *Phys. Rev. E*, 72, 046301
- Barnes, A. 1983, in *Solar-Terrestrial Physics: Principles and Theoretical Foundations* (Dordrecht: Reidel), 155
- Biskamp, D., & Müller, W.-C. 2000, *Phys. Plasmas*, 7, 4889
- Boldyrev, S., Mason, J., & Cattaneo, F. 2006, preprint (astro-ph/0605233)
- Borini, G., Gosling, J. T., Bame, S. J., & Feldman, W. D. 1983, *Sol. Phys.*, 83, 367
- Bruno, R., & Carbone, V. 2005, *Living Rev. Sol. Phys.*, 2, 4
- Burlaga, L. F. 1995, *Interplanetary Magnetohydrodynamics* (New York: Oxford Univ. Press)
- Cho, J., & Vishniac, E. T. 2000, *ApJ*, 539, 273
- Goldstein, B. E., Smith, E. J., Balogh, A., Horbury, T. S., Goldstein, M. L., & Roberts, D. A. 1995, *Geophys. Res. Lett.*, 22, 3393
- Goldstein, M. L., Roberts, D. A., Deane, A. E., Ghosh, S., & Wong, H. K. 1999, *J. Geophys. Res.*, 104, 14437
- Haugen, N. E. L., & Brandenburg, A. 2004, *Phys. Rev. E*, 70, 036408
- Haugen, N. E. L., Brandenburg, A., & Dobler, W. 2003, *ApJ*, 597, L141
- . 2004a, *Phys. Rev. E*, 70, 016308
- . 2004b, *Ap&SS*, 292, 53
- Leamon, R. J., Smith, C. W., Ness, N. F., Matthaeus, W. H., & Wong, H. K. 1998, *J. Geophys. Res.*, 103, 4775
- Lepping, R. P., et al. 1995, *Space Sci. Rev.*, 71, 207
- Lin, R. P., et al. 1995, *Space Sci. Rev.*, 71, 125
- Maron, J., & Goldreich, P. 2001, *ApJ*, 554, 1175
- Marsch, E. 1991, in *Physics of the Inner Heliosphere II. Particles, Waves, and Turbulence*, ed. R. Schwenn & E. Marsch (Berlin: Springer), 159
- Marsch, E., & Tu, C.-Y. 1990, *J. Geophys. Res.*, 95, 8211
- Mason, J., Cattaneo, F., & Boldyrev, S. 2006, *Phys. Rev. Lett.*, 97, 255002
- Matthaeus, W. H., & Goldstein, M. L. 1982, *J. Geophys. Res.*, 87, 6011
- Mininni, P., Alexakis, A., & Pouquet, A. 2005, *Phys. Rev. E*, 72, 046302
- Mininni, P. D., & Montgomery, D. C. 2005, *Phys. Rev. E*, 72, 056320
- Müller, W.-C., & Biskamp, D. 2000, *Phys. Rev. Lett.*, 84, 475
- Müller, W.-C., Biskamp, D., & Grappin, R. 2003, *Phys. Rev. E*, 67, 066302
- Müller, W.-C., & Grappin, R. 2005, *Phys. Rev. Lett.*, 95, 114502
- Percival, D. B., & Walden, A. T. 1993, *Spectral Analysis for Physical Applications* (Cambridge: Cambridge Univ. Press)
- Podesta, J. J. 2006, *J. Geophys. Res.*, 111, A07103
- Podesta, J. J., Roberts, D. A., & Goldstein, M. L. 2006, *J. Geophys. Res.*, 111, A10109
- Roberts, D. A., Goldstein, M. L., & Klein, L. W. 1990, *J. Geophys. Res.*, 95, 4203
- Roberts, D. A., Klein, L. W., Goldstein, M. L., & Matthaeus, W. H. 1987, *J. Geophys. Res.*, 92, 11021
- Tu, C.-Y., & Marsch, E. 1995, *Space Sci. Rev.*, 73, 1
- Verma, M. K., Roberts, D. A., Goldstein, M. L., Ghosh, S., & Stribling, W. T. 1996, *J. Geophys. Res.*, 101, 21619